

Fluorescence-dip infrared spectroscopy of the tropolone-H₂O complex

Rex K. Frost, Fredrick C. Hagemester, Caleb A. Arrington, David Schleppebach,
and Timothy S. Zwier^{a)}

Department of Chemistry, Purdue University, West Lafayette, Indiana 47907-1393

Kenneth D. Jordan^{a)}

Department of Chemistry, University of Pittsburgh, Pittsburgh, Pennsylvania 15260

(Received 13 March 1996; accepted 7 May 1996)

Fluorescence dip infrared spectroscopy (FDIRS) is used to probe the effect of a solvent water molecule on intramolecular H-atom tunneling in tropolone. As with the bare molecule discussed in paper I, the FDIR spectrum of the tropolone-H₂O complex is recorded in the O-H and C-H stretch regions. Three OH stretch fundamentals are observed in the spectrum, and can be assigned nominally to a free OH stretch of the water molecule (3724 cm⁻¹), a hydrogen bonded OH stretch of water (3506 cm⁻¹), and the OH stretch of tropolone (~3150 cm⁻¹). The breadth and complexity of the bands is highly mode specific. The free OH stretch transition is sharp (1.8 cm⁻¹ FWHM) and has weak combination bands built on it at +73 and +1600 cm⁻¹. The former is assigned to a combination band with the in-plane bending mode of the tropolone-H₂O hydrogen bond, while the latter is the free OH/intramolecular water bend combination band. The water hydrogen-bonded OH fundamental is also a sharp transition which, after correction for the decreased infrared power at its frequency, is clearly the strongest transition in the spectrum. It is flanked by three close-lying satellite bands 13, 23, and 34 cm⁻¹ above it, and also supports a weak combination band at +69 cm⁻¹ due to the in-plane intermolecular bending mode. The tropolone OH absorption is in the same frequency region as in the bare molecule, but broadened to over 100 cm⁻¹ in TrOH-H₂O. Distinct substructure in the band is present, with spacings reminiscent of those in the water H-bonded OH stretch region. *Ab initio* calculations on tropolone-H₂O are carried out at both the MP2 and Becke3LYP levels of theory. Two isomers with similar binding energies and vibrational frequencies are identified. In one isomer (isomer I), the water molecule serves as a hydrogen-bonded bridge between the tropolone OH and keto groups. In the other (isomer II), the water molecule is exterior to the tropolone and hydrogen bonded to the keto oxygen. The experimental evidence does not conclusively distinguish between these two possibilities, though the exterior structure seems somewhat more in keeping with the data as a whole. © 1996 American Institute of Physics. [S0021-9606(96)01831-4]

I. INTRODUCTION

The sensitivity of a solute molecule to the position and nature of a solvent molecule is particularly great in a molecule such as tropolone which can undergo intramolecular H-atom tunneling in a symmetric double minimum potential well. In the most dramatic case, a single solvent molecule binding in a distinctly asymmetric position can completely quench the tunneling, even if it is facile in the absence of solvent.

Due to the hydrogen-bonding capacity of H₂O, it is anticipated that its complexation to tropolone will occur in the region where H-atom transfer occurs. Given the amphoteric character of water and the presence of both keto and OH groups on tropolone, several modes of binding of water to tropolone can be envisioned, and each will have a distinctly different effect on the H-atom tunneling coordinate. Furthermore, as a protic solvent, the possibility exists that water may play an active role in mediating H-atom transfer with tropolone.

Cursory studies¹ of the $S_1 \leftarrow S_0$ spectroscopy of

TrOH-H₂O carried out in the past show no evidence of tunneling splittings in the spectra, indicating that in the levels probed, H-atom tunneling in tropolone is effectively quenched by the water molecule. In parallel with our work, Sekiya and co-workers² have carried out a dispersed fluorescence study of several vibronic bands of TrOH-H₂O, including an experimental and cursory *ab initio* investigation of the intermolecular vibrational frequencies and isomeric structures of the complex. Nonetheless, the structure of the complex and the spectroscopy and dynamics of the OH stretching modes are largely unexplored. Furthermore, the complexation of water to tropolone juxtaposes the spectral properties of intramolecular and intermolecular hydrogen bonds in the same complex. Both these subjects form the basis of the present study, employing fluorescence-dip infrared spectroscopy (FDIRS).

The following paper by Mitsuzuka *et al.*³ reports results of their analogous study of tropolone-(H₂O)_n and tropolone-(CH₃OH)_n clusters. Due to the higher power optical parametric oscillator (OPO) and different experimental implementation in our work, the spectra reported herein include those in the tropolone OH stretch region, which is

^{a)}Authors to whom correspondence should be addressed.

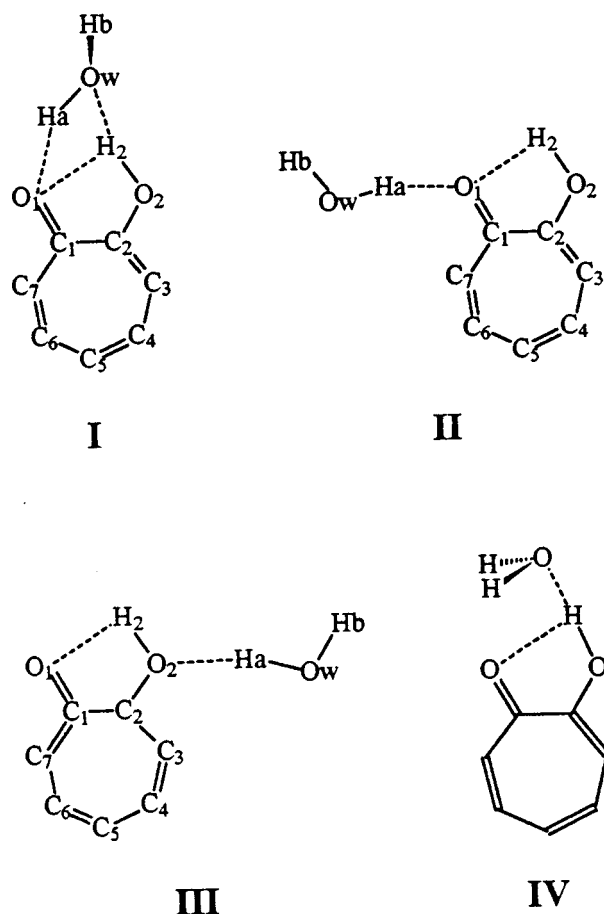


FIG. 1. Several potential structures for the tropolone-H₂O complex. Of these structures, I–III support potential minima, while structure IV rearranges to structure I upon optimization.

characterized by broad, weak absorptions which are thereby hard to detect. As a result, we have focused attention on the tropolone-H₂O complex, while the work of Mitsuzuka *et al.*³ provides an important extension to larger tropolone-(H₂O)_n clusters, to tropolone-(CH₃OH)_n clusters, and to the *S*₁-state OH stretch infrared spectrum of the tropolone-H₂O complex.

Finally, as a part of the present study, we have carried out extensive *ab initio* calculations on the tropolone-H₂O complex. Several isomeric structures have been explored by *ab initio* methods following a first sifting of 15 possible structures for the complex using semiempirical methods. Not surprisingly, the lowest energy structures are consistently those in which the tropolone retains at least some degree of its intramolecular hydrogen bond. Several of these are shown schematically in Fig. 1. Structures I–III are minima while structure IV, identified as a minimum in previous work⁴ using semiempirical methods, rearranges to structure I upon optimization in the *ab initio* calculations. Structures I and II (hereafter referred to as the ring and exterior isomers, respectively) have binding energies considerably greater than III, and nearly equal to one another. Vibrational frequencies and intensities for these two isomers have been calculated and serve as the basis for comparison with experiment.

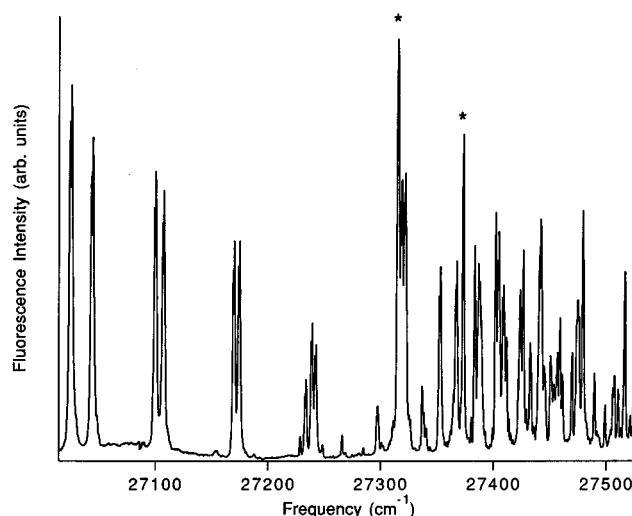


FIG. 2. Fluorescence excitation spectrum of TrOH and TrOH-H₂O. The origin and first strong intermolecular transitions of TrOH-H₂O are marked by asterisks. These serve as monitor transitions for the fluorescence-dip infrared spectroscopy. The latter band was typically used due to its small overlap with TrOH transitions.

II. EXPERIMENT

The method of fluorescence-dip infrared spectroscopy (FDIRS) used by our group has been discussed in the preceding paper, to which the reader is referred for details.⁵ In addition, infrared-ultraviolet hole burning spectroscopy is used here to obtain the electronic spectrum of the tropolone-H₂O complex free from interference from tropolone's spectrum, in which it is intermingled. IR-UV hole burning is also applied by Mitsuzuka *et al.*³ to tropolone-H₂O in the following paper. Our application of this method employs the same scheme for detection as in FDIRS; namely, the use of active baseline subtraction. Its application to hole burning spectroscopy is analogous to the ultraviolet-ultraviolet hole burning methods employed by our group on 5-hydroxytropolone.^{6,7} The infrared OPO, operating at a repetition rate of 20 Hz, is fixed on an infrared resonance of TrOH-H₂O identified by FDIRS. The ultraviolet laser, operating at 40 Hz, is then tuned through the vibronic transitions of the complex. The gated integrator used for detection then records the difference in fluorescence signal without and with the infrared OPO present, using active baseline subtraction.

In forming the tropolone-H₂O complex, trace amounts of water (~0.1% in helium) are added to the helium expansion, flowing over a room temperature or slightly heated tropolone sample (~40 °C).

III. RESULTS

The *S*₁←*S*₀ transition typically used to monitor the tropolone-H₂O complex is 57 cm⁻¹ above the *S*₁ origin and is marked by an asterisk in Fig. 2. This transition involves an intermolecular vibration built on the origin of tropolone-H₂O (also marked in the figure), and was chosen largely because it is free from interference from tropolone bands, though

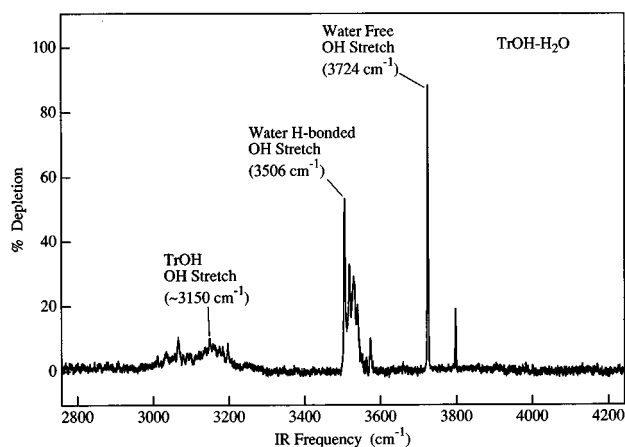


FIG. 3. Overview FDIR spectrum of the tropolone-H₂O complex.

identical spectra were obtained by monitoring the origin transition. Earlier work has assigned these bands to the tropolone-H₂O complex,¹ and this is confirmed by our work and by the hole burning spectroscopy of Mitsuzuka *et al.*³ presented in the following paper. The lack of observable tunneling splittings in the $S_1 \leftarrow S_0$ vibronic transitions of tropolone-H₂O indicates that the water molecule has reduced the tunneling splittings for symmetric tunneling routes to below 1 cm^{-1} so that they are unresolved at the present resolution.

A. Fluorescence-dip infrared spectra

An overview FDIR spectrum of tropolone-H₂O extending from 2800 to 4200 cm^{-1} is shown in Fig. 3. The spectrum shows absorptions in three regions near 3700, 3500, and 3100 cm^{-1} . Striking differences exist between the appearance of the absorptions in these three regions; particularly in the breadths and the substructure of the bands. A qualitative assignment of these features can be made immediately. The dominant peak in the high frequency region is the sharp band at 3724 cm^{-1} . This is assigned as a free OH stretch. Molecular clusters containing water often have absorptions assignable to free OH. In (H₂O)₂, the free OH stretch of the donor water molecule⁸ is at 3730 cm^{-1} while in benzene-(H₂O)_n clusters with $n=3-7$ such absorptions are found in the 3715–3725 cm^{-1} region.⁹⁻¹² The free OH stretch bands appear at this frequency because the formation of a strong H bond with one OH in water reduces the intramolecular OH–OH coupling. The water symmetric and asymmetric stretch modes are then best described as local mode free and H-bonded OH vibrations. The free OH then has a frequency corresponding to an uncoupled OH bond, halfway between the symmetric (3657 cm^{-1}) and asymmetric stretch (3756 cm^{-1}) of water.

The set of bands at 3500 cm^{-1} are assigned to the water hydrogen-bonded donor OH. For comparison, the water–water H-bonded OH transitions in benzene-(H₂O)₂ (Refs. 10–12) and fluorobenzene-(H₂O)₂ (Ref. 13) are assigned to bands at 3550 and 3547 cm^{-1} , respectively.

Finally, as will be confirmed on closer inspection in a

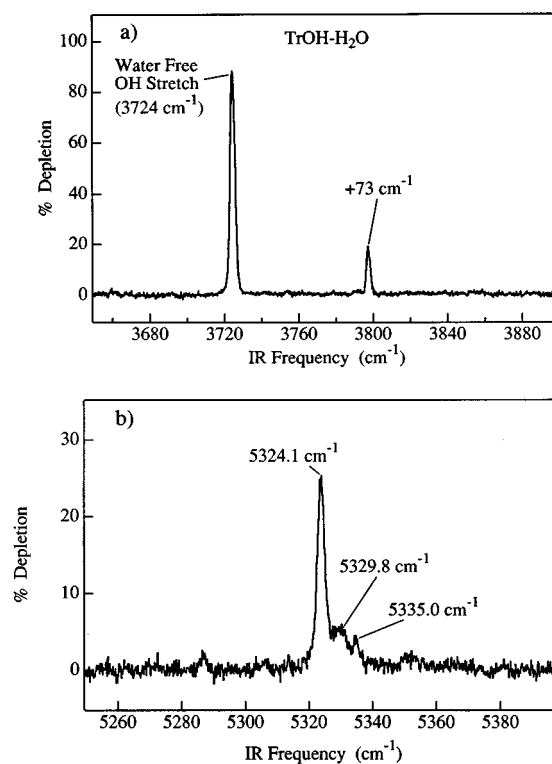


FIG. 4. Close up FDIR spectra (a) of the free OH stretch region, and (b) of the free OH/intramolecular water bending combination band of tropolone-H₂O.

moment, the broad band centered on 3100 cm^{-1} contains several C–H stretch transitions and the intramolecularly H-bonded OH stretch of tropolone. As was shown in the preceding paper,⁵ in bare tropolone the main O–H transitions are found at 3134 and 3135 cm^{-1} .

Figure 4(a) shows an expanded view of the free OH stretch region in tropolone-H₂O. The spectrum in this region is dominated by a single peak at 3724 cm^{-1} in which the ground state population can be over 90% depleted by the infrared OPO. This indicates that the cluster predissociates following vibrational excitation, allowing greater than 50% depletion to occur. The peak is quite sharp, with width determined by a convolution of the rotational band contour with the OPO bandwidth. When plotted as an absorbance (i.e., on a logarithmic scale), the peak is 1.8 cm^{-1} full width at half maximum.

Two weak, sharp combination bands are built on the free OH stretch transition. The first is at 3797 cm^{-1} , 73 cm^{-1} above the free OH fundamental, and must involve an intermolecular vibration of the complex. A tentative assignment of this vibration as the in-plane bend of the water molecule will be supported in the discussion section.

The second combination band, at 5324 cm^{-1} , is shown in Fig. 4(b). It was initially observed in experiments in which both signal and idler beams from the OPO were used in the FDIR scan. Subsequent scans with a filter in place to remove the signal beam also removed this absorption, identifying it as arising from the higher frequency signal beam at 5324 cm^{-1} . The sharpness of the band suggests that it is built off

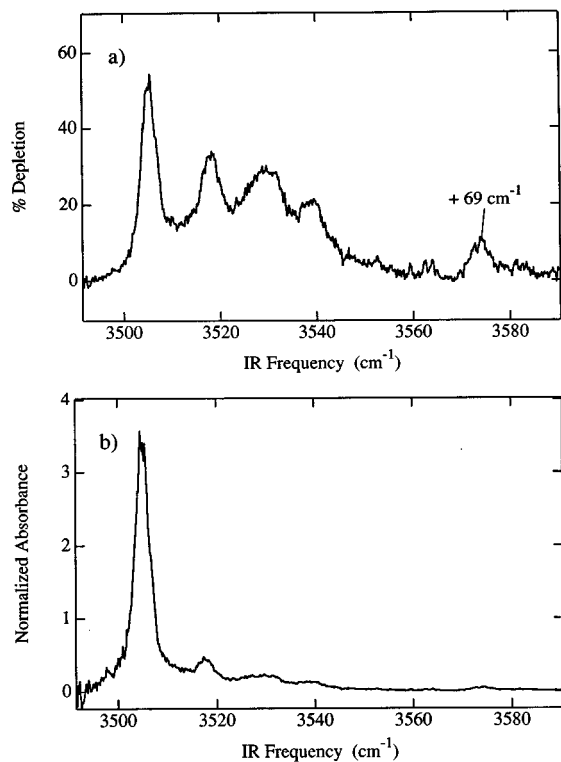


FIG. 5. Close up FDIR spectrum of the water H-bonded OH stretch region (a) as an unpower-normalized percent depletion, and (b) as a power-normalized absorbance. The spectrum in (a) is distorted in intensity due to the steeply decreasing OPO power in the region 3510–3490 cm^{-1} due to an impurity absorption in the LiNbO₃ crystal.

the free OH stretch, and would thereby have a fundamental frequency of 1600 cm^{-1} . Since the bending fundamental of H₂O is at 1595 cm^{-1} , we assign this combination band as a water free OH/water bending combination band.

Figure 5(a) shows an expanded view of the spectrum in the 3500 cm^{-1} region assigned to the H-bonded OH stretch of the water molecule. Under this closer inspection, the region is composed of a total of five transitions at frequencies 13.0, 24.8, 33.4, and 69 cm^{-1} above the fundamental. The spectrum of Fig. 5(a) is misleading in one important respect; namely, that the lowest frequency band located at 3506 cm^{-1} is significantly reduced in intensity due to the band's position right on the edge of a narrow (3470–3510 cm^{-1}), but significant drop in the LiNbO₃ OPO power intensity. As pointed out by Ebata *et al.*,¹⁴ the infrared absorption cross section in a depletion experiment of the present type is given by

$$\sigma_{\text{abs}} = -\frac{\ln\left(\frac{C_{\text{on}}}{C_{\text{off}}}\right)}{I_{\text{IR}}\Delta t} = -\frac{\ln\left(1 - \frac{\% \text{ dip}}{100}\right)}{I_{\text{IR}}\Delta t},$$

where C_{on} and C_{off} are the ion intensities on and off resonance with the infrared OPO whose intensity and duration are I_{IR} and Δt . Figure 5(b) is an infrared power-normalized version of the spectrum, plotted on the logarithmic scale as a relative absorbance. Note that on this basis, the water

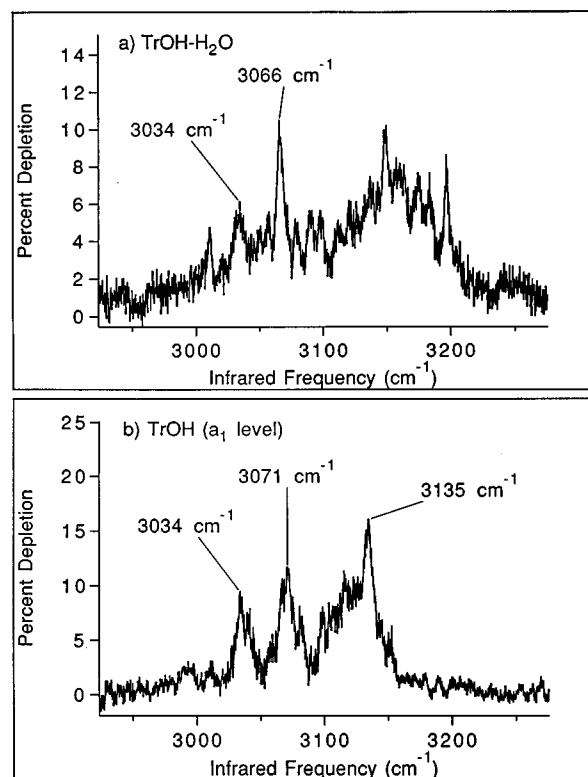


FIG. 6. FDIR spectra in the tropolone OH stretch region for (a) the tropolone-H₂O complex, and (b) the lower member of the zero-point tunneling doublet in tropolone (of a_1 symmetry).

H-bonded OH stretch fundamental dominates the spectrum, and is several times the size of the free OH band at 3724 cm^{-1} .

A discussion of the possible sources of the close-lying sidebands will be given in Sec. V, but some brief comments are in order here. First, these sidebands cannot be sequence bands because we are monitoring a cold band in the fluorescence spectrum in recording the infrared spectrum. Second, several of the transitions are too close to the water H-bonded OH fundamental to be combination bands built on that fundamental. Third, the region of low OPO power precludes our making a careful investigation of whether similar bands exist on the low frequency side of the fundamental.

The broad set of bands in the 3100 cm^{-1} region of TrOH-H₂O is shown on an expanded frequency scale in Fig. 6(a), with the corresponding spectrum of a_1 symmetry tropolone shown below it for comparison [Fig. 6(b)]. On this scale it is apparent that the broad absorptions are a composite of a large number of bands spread over almost 200 cm^{-1} . The bands at 3034 and 3065 cm^{-1} in the spectrum of TrOH-H₂O bare a close correspondence with the bands at 3034 and 3071 cm^{-1} in TrOH, which were assigned in the preceding paper as C–H stretch absorptions. This is consistent with the expectation that the C–H stretch frequencies should not be changed by the presence of the water molecule in the complex.

In the preceding paper,⁵ the OH stretch fundamental of TrOH(a_1) is assigned to the band at 3134.9 cm^{-1} in Fig.

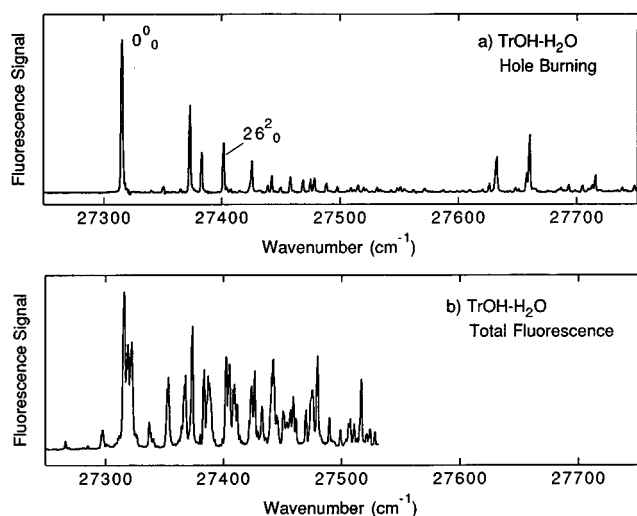


FIG. 7. (a) Infrared-ultraviolet hole-burning spectroscopy of tropolone-H₂O in the same region using the 3724 cm⁻¹ band as infrared hole-burning wavelength. (b) Fluorescence excitation spectrum of tropolone and tropolone-H₂O in the region of the S₁←S₀ origin.

6(b). By comparison, the broad, structured absorption in TrOH-H₂O centered at 3150 cm⁻¹ is also assigned to bands whose oscillator strength is derived from tropolone's OH stretching mode. Therefore, the binding of water to tropolone has little effect on the absorption frequency or intensity of the tropolone OH stretch, but significantly changes the breadth and substructure of the band.

B. Infrared-ultraviolet hole burning spectroscopy

The clear study of the electronic spectroscopy of tropolone-H₂O is hindered by the interspersal of its transitions among the intense vibronic bands of the tropolone monomer. In order to selectively view the transitions of the tropolone-H₂O complex, infrared-ultraviolet hole burning spectroscopy has been employed with the saturating infrared OPO source tuned to either the 3724 or 3506 cm⁻¹ transitions of the complex. A similar study has been carried out by Mitsuzuka *et al.*³ in the following paper, so that only a brief account is given here. The resulting IR-UV hole burning spectrum of the first 400 cm⁻¹ above the S₁←S₀ origin is shown in Fig. 7(a). Below it is shown the fluorescence excitation spectrum of the same region in order to highlight the excellent discrimination of the method. From comparison of the spectrum with that of tropolone, it is clear that extensive intermolecular structure is present in the spectrum of the complex, though saturation of the ultraviolet transitions magnifies the relative intensities of the intermolecular bands in the present experiment. Most of the observed transitions can be accounted for as overtones and combination bands of three transitions at 57, 67, and 86 cm⁻¹. Sekiya and co-workers² have recently assigned these three bands based on a comparison of their dispersed emission spectra with *ab initio* frequency calculations at the HF 6-31G** level. The

86 cm⁻¹ transition is assigned as 26₀², while the 57 and 67 cm⁻¹ bands are an intermolecular bend and the intermolecular stretch, respectively.

IV. AB INITIO CALCULATIONS

Ab initio calculations were carried out on the tropolone-H₂O complex to determine (i) which structures are minima in the intermolecular potential energy surface, (ii) the binding energies for these structures, and (iii) the vibrational frequencies and infrared intensities of the lowest energy isomers for comparison with experiment.

A. Isomeric structures and their binding energies

One of the computational problems posed by the tropolone-H₂O complex is the existence of multiple potential energy minima. *Ab initio* electronic structure calculations can prove particularly valuable for providing information on the number and structures of the low-lying minima and on the heights of the barriers for interconversion between minima. As in the study of tropolone in the preceding paper, we have employed¹⁵ both second-order many-body perturbation theory (MP2)¹⁶ and density functional theory using the Becke3LYP nonlocal exchange-correlation functional.¹⁷ The basis sets used were the same as employed in the calculations on tropolone in the preceding paper; namely, 6-31+G* for survey calculations and 6-31+G'[2d,p] for more accurate Becke3LYP and MP2 calculations. The details of these basis sets are described in the preceding paper.

Of the four possible structures presented in Fig. 1, structures I–III are found to be local minima in the Becke3LYP/6-31+G* calculations, whereas IV collapsed back to structure III. Structure III is predicted to be over 2 kcal/mol less stable than structures I and II. Therefore, only the latter two structures (hereafter called the “ring” and “exterior” isomers) are considered in the calculations employing the 6-31+G'[2d,p] basis set, with their geometries optimized with both the Becke3LYP and MP2 methods.

Perhaps the greatest hurdle in calculating accurate binding energies of hydrogen-bonded clusters is posed by the basis set superposition error (BSSE),¹⁸ an artifact due to the use of finite basis sets. This results from the improved description of one molecule in the cluster by the use of basis functions on the other molecule(s). Counterpoise corrections¹⁸ for BSSE are obtained by calculating the energy of the water monomer with the geometry it has in the complex both in the presence of [E*(H₂O)] and in the absence of [E(H₂O)] the basis functions of tropolone. Similarly, calculations are carried out on tropolone (with the structure it has in the complex) both in the presence of [E*(tropolone)] and in the absence of [E(tropolone)] basis functions on the water molecule. The total BSSE correction for tropolone-H₂O is then given by

$$\text{BSSE}(\text{corr}) = E(\text{H}_2\text{O}) - E^*(\text{H}_2\text{O}) + E(\text{tropolone}) - E^*(\text{tropolone}).$$

Table I summarizes the key structural parameters for the ring and exterior isomers, while Fig. 8 shows the structures

TABLE I. Key bond lengths r (Å) and bond angles a (degrees) for the calculated TrOH structure and the two lowest-energy TrOH-H₂O (1:1) conformational isomers.

	TrOH		TrOH-H ₂ O (ring)		TrOH-H ₂ O (exterior)	
	Becke3LYP ^a	MP2 ^b	Becke3LYP ^a	MP2 ^b	Becke3LYP ^a	MP2 ^b
$r_{C_1-O_1}$	1.254 (1.249)	1.260	1.255 (1.249)	1.260	1.264 (1.258)	1.269
$r_{C_2-O_2}$	1.337 (1.330)	1.337	1.333 (1.328)	1.335	1.337 (1.331)	1.338
$r_{O_1-O_2}$	2.507 (2.486)	2.501	2.670 (2.666)	2.661	2.502 (2.488)	2.498
$r_{O_2-H_2}$	0.995 (0.993)	0.995	0.994 (0.990)	0.990	0.993 (0.990)	0.994
$r_{O_1-H_2}$	1.828 (1.789)	1.795	2.212 (2.206)	2.166	1.830 (1.804)	1.799
$r_{O_1-H_a}$			1.881 (1.836)	1.886	1.868 (1.874)	1.876
$r_{O_2-H_a}$			2.861 (2.802)	1.889	4.369 (4.358)	4.372
$r_{O_1-O_w}$			2.706 (2.694)	2.718	2.818 (2.824)	2.818
$r_{O_2-O_w}$			2.778 (2.775)	2.801	5.320 (5.312)	5.312
$r_{H_a-O_w}$			0.980 (0.978)	0.976	0.981 (0.976)	0.977
$r_{O_w-H_b}$			0.969 (0.963)	0.964	0.968 (0.962)	0.963
$a_{C_1-C_2-O_2}$	111.6 (111.2)	111.6	116.7 (116.6)	116.6	112.2 (111.8)	112.2
$a_{C_2-C_1-O_1}$	114.8 (114.6)	115.1	117.9 (118.1)	118.1	114.2 (114.1)	114.5
$a_{C_2-O_2-H_2}$	103.9 (103.0)	102.1	114.1 (113.9)	111.9	104.2 (103.5)	102.4
$a_{O_2-H_2-O_1}$	122.4 (124.1)	124.8	106.5 (106.8)	109.1	122.0 (123.2)	124.3
$a_{O_w-H_a-O_1}$			140.0 (144.7)	141.4	162.1 (163.6)	161.0
$a_{O_2-H_2-O_w}$			169.2 (169.1)	165.5	132.5 (134.8)	133.6

^aStructural parameters are given for the 6-31+G* basis set calculation, with the 6-31+G'[2*d*,*p*] set results in parentheses.

^bStructural parameters are given for the 6-31+G[2*d*,*p*] basis set calculation.

pictorially. Rotational constants and binding energies for the two isomers and for tropolone are given in Table II. The binding energies are given both with and without corrections for BSSE and zero-point energy (where possible). As is evident from Table II, both Becke3LYP and MP2 calculations predict slightly larger binding energies for isomer II (the ‘‘exterior water’’ isomer) than for isomer I (the ‘‘ring’’ isomer) both with and without corrections for BSSE and ZPE. Nevertheless, the energy difference between the two structures is not large, and one cannot on this basis alone favor one isomer over the other in comparing with the present experiment. Furthermore, it should be noted that both struc-

tures meet the general criteria posed by the experimental spectrum of possessing a free OH group, a H-bonded water OH, and a tropolone OH.

The ring isomer is perhaps most interesting from a structural viewpoint. Figure 9 compares the structures of tropolone and the ring structure of tropolone-H₂O at the 6-31+G'[2*d*,*p*] level of theory. Clearly, the major structural change in tropolone is in the opening of the COH bond angle by 10.9° in the presence of water. This leads to a 0.18 Å larger O–O separation in isomer I than in tropolone. The reason for these changes is obvious: the tropolone OH weakens its intramolecular H bond in order to simultaneously form a second hydrogen bond with the water molecule. One of the water molecule's OH groups, in turn, hydrogen bonds to the keto oxygen to form a strained, 7-membered ring structure with water as bridge while the 5-membered intramolecular ring is still largely intact, but perhaps weakened.

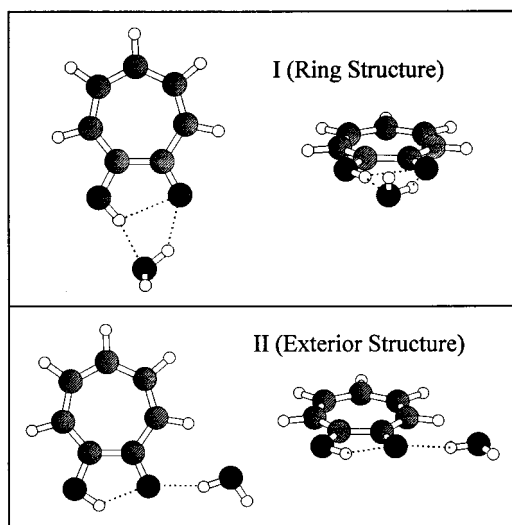


FIG. 8. The ring (upper panel) and exterior (lower panel) conformational isomers of TrOH-H₂O calculated at the Becke3LYP/6-31+G[2*d*,*p*] level of theory.

B. Infrared frequencies, intensities, and mode mixings

Table III presents the experimental and calculated harmonic vibrational frequencies and infrared intensities for the tropolone monomer and the exterior and ring isomers of TrOH-H₂O using Becke3LYP functionals with a 6-31+G* and 6-31+G'[2*d*,*p*] basis sets. Prior work on water clusters and benzene-(H₂O)_{*n*} clusters has shown that the Becke3LYP and MP2 methods give similar values for the frequency shifts of the OH stretch modes.¹⁹ The vibrational frequencies were also used to compute zero-point energies, thus enabling energy differences to be computed with ZPE corrections.

A primary point of comparison with experiment is via the frequency shift that the intramolecular vibrations of

TABLE II. Calculated binding energies^a of three TrOH-H₂O (1:1) conformational isomers.

	I (ring structure)	II (exterior structure)	III
Becke3LYP/6-31+G*	-7.74	-7.82	-5.25
Becke3LYP/6-31+G* _w /ZPE ^b	-5.64	-5.68	
Becke3LYP/6-31+G'[2 <i>d,p</i>]	-6.08	-6.50	
Becke3LYP/6-31+G'[2 <i>d,p</i>] _w /ZPE ^b	-4.21	-4.79	
Becke3LYP/6-31+G'[2 <i>d,p</i>] _w /ZPE ^b & BSSE ^c	-3.58	-4.32	
MP2/6-31+G'[2 <i>d,p</i>]	-7.15	-7.82	
MP2/6-31+G'[2 <i>d,p</i>] _w /ZPE ^d	-5.28	-6.11	
MP2/6-31+G'[2 <i>d,p</i>] _w /ZPE ^d & BSSE ^c	-3.69	-4.99	
Rotational constants	2.6577	1.8201	
(in GHz)	0.8285	0.9637	
calculated at MP2/6-31+G'[2 <i>d,p</i>]	0.6326	0.6301	

^aEnergies are given in units of kcal/mol with wave number equivalent units in parentheses.

^bZero-point energy level corrected energies.

^cCounter-poise BSSE corrected energies.

^dZero-point energy corrections taken from the Becke3LYP/6-31+G'[2*d,p*] level of theory.

tropolone and water undergo in the tropolone-H₂O complex. In order to facilitate such a comparison, the overlap coefficients between the normal modes of the monomers and the complex have been computed. In the great majority of cases, an excellent one-to-one correspondence exists. However, in a few cases, there are significant mixings of normal modes in forming the complex. Table IV lists the mode mixings in several of the modes of relevance to the following discussion. An obvious effect of complexation is the localization of the symmetric and antisymmetric stretch modes of water into free OH and water H-bonded OH, as already anticipated. In a local mode basis set, the OH stretch modes are calculated to be 99.8%/97.7%/97.5% localized in the TrOH OH, water donor OH and water free OH of the interior isomer, while in the exterior isomer the corresponding localizations are 99.0%/95.4%/96.2%. In the ring structure, the close interaction of the water molecule to the C=O...HO of tropolone creates larger mode mixing in several of tropolone's modes in this isomer.

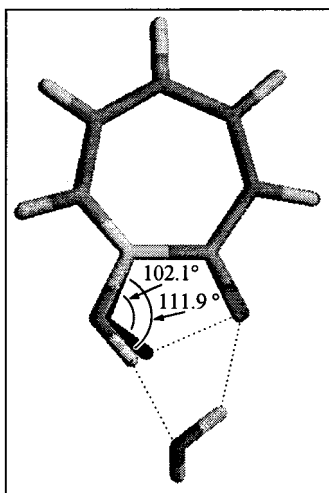


FIG. 9. An overlay of the structures of tropolone and of tropolone in the ring isomer of TrOH-H₂O highlighting the opening of the chelating C=O/OH on tropolone with water present.

V. DISCUSSION

A. The experimentally probed TrOH-H₂O isomer

The calculations have identified two conformers of tropolone-H₂O which are near in energy to one another and which also meet the general criteria of having one free OH, one water H-bonded OH, and a largely intact intramolecularly H-bonded OH on tropolone. In this section, the harmonic vibrational frequencies and infrared intensities calculated for each isomer are compared with experiment with the goal of distinguishing which isomer is being probed in the present experiment. We will see, in the final analysis, that while the data may show a slight preference for one isomer over the other, no definite answer to this question can be given based on the present experimental data.

The experimental data available for distinction between the two conformers is considerable. These include the $S_1 \leftarrow S_0$ electronic frequency shift, vibrational frequency shifts of water and tropolone intramolecular vibrations, intermolecular vibrational frequencies, OH stretch and CH stretch infrared intensities, the comparison with previously studied systems, and simple chemical intuition. Table V lists the vibrational frequency shifts of a subset of vibrations where direct comparison between theory and experiment can be made. The three normal modes of water are considered at the top of the table while a selection of tropolone's modes are shown below it. We have included in the table several vibrations which are not directly probed in the present experiment, but whose frequencies are available from the recent dispersed emission spectra of TrOH-H₂O by Sekiya *et al.*²

1. Evidence supporting either isomer

Several comparisons between experiment and calculation are surprisingly inconclusive in distinguishing which structure is the experimentally probed complex.

(a) The OH stretch vibrational frequency shifts calculated for the two isomers are not very different (+8, -267, and +13 cm⁻¹ for the ring structure compared to +23, -277, and +54 cm⁻¹ for the exterior isomer at the Becke3LYP/6-31+G'[2*d,p*] level). The free OH vibrational

TABLE III. Calculated frequencies and intensities for TrOH, H₂O, and both the ring and exterior TrOH H₂O complexes.^a

Mode number	TrOH		Mode number	Ring isomer of TrOH-H ₂ O		Exterior isomer of TrOH-H ₂ O	
	Frequency	Intensity		Frequency	Intensity	Frequency	Intensity
1	114.9 (120.6)	1.1 (1.0)	1	49.6 (49.8)	5.3 (4.2)	41.8 (-44.6)	0.0 (126.9)
2	185.1 (183.8)	0.0 (0.0)	2	84.1 (87.0)	1.7 (1.4)	68.7 (35.7)	15.8 (5.9)
3	363.4 (358.6)	6.1 (10.1)	3	144.1 (118.1)	16.1 (10.4)	101.1 (62.9)	150.2 (12.2)
4	373.9 (370.4)	4.8 (2.7)	4	174.6 (167.3)	18.7 (30.1)	119.4 (120.0)	18.5 (0.1)
5	376.1 (377.8)	0.0 (0.0)	5	183.4 (181.9)	3.0 (2.2)	166.4 (150.7)	3.5 (5.4)
6	402.2 (403.9)	1.8 (2.1)	6	299.9 (317.0)	157.6 (165.4)	187.7 (184.3)	0.1 (0.0)
7	448.4 (445.6)	15.0 (15.2)	7	329.5 (325.5)	32.6 (37.8)	368.3 (366.2)	0.7 (16.0)
8	545.9 (549.8)	1.8 (1.9)	8	358.3 (358.6)	56.5 (28.3)	381.6 (368.5)	54.6 (53.9)
9	597.6 (601.9)	0.2 (0.1)	9	373.9 (374.9)	6.7 (5.5)	382.4 (381.1)	0.4 (0.2)
10	694.2 (693.8)	7.3 (6.5)	10	382.6 (380.0)	49.2 (35.6)	406.9 (406.0)	3.3 (3.0)
11	724.8 (739.5)	19.6 (33.5)	11	402.9 (404.8)	0.1 (0.2)	438.6 (424.4)	179.4 (139.2)
12	751.5 (751.9)	14.3 (14.5)	12	455.6 (457.0)	6.7 (3.2)	457.6 (452.0)	52.0 (32.3)
13	773.2 (783.0)	79.7 (51.5)	13	539.3 (540.8)	46.9 (47.4)	558.8 (559.5)	1.5 (2.0)
14	814.8 (849.7)	76.7 (58.1)	14	600.9 (604.5)	0.5 (0.2)	601.7 (603.0)	0.0 (0.2)
15	878.4 (885.1)	10.3 (10.1)	15	648.0 (650.0)	337.0 (298.2)	660.3 (623.3)	75.4 (56.0)
16	888.4 (885.3)	10.8 (10.5)	16	696.7 (693.9)	22.6 (14.7)	700.6 (699.4)	6.2 (6.0)
17	945.0 (941.7)	11.2 (11.6)	17	722.6 (738.3)	29.1 (50.4)	734.6 (745.2)	31.9 (34.6)
18	977.5 (973.2)	10.3 (9.9)	18	751.5 (750.6)	24.9 (21.6)	752.1 (752.0)	22.2 (21.7)
19	1014.2 (1012.3)	0.3 (0.2)	19	771.4 (781.1)	74.7 (43.2)	776.2 (782.3)	82.6 (65.4)
20	1030.2 (1028.8)	1.1 (1.1)	20	863.4 (864.1)	31.0 (41.0)	802.8 (823.9)	84.6 (54.4)
21	1080.6 (1077.1)	0.4 (0.4)	21	890.4 (887.8)	6.9 (6.6)	891.6 (888.0)	9.9 (11.7)
22	1244.6 (1236.8)	7.8 (4.5)	22	911.0 (901.8)	106.9 (52.3)	891.6 (892.6)	12.0 (4.5)
23	1248.9 (1241.9)	7.5 (7.3)	23	952.9 (950.3)	1.6 (3.2)	956.2 (951.3)	14.6 (12.0)
24	1294.1 (1282.3)	44.8 (32.0)	24	990.5 (987.2)	12.9 (11.6)	983.7 (978.9)	9.9 (9.8)
25	1324.9 (1320.7)	223.5 (203.1)	25	1014.6 (1013.7)	0.2 (0.2)	1017.8 (1015.6)	0.1 (0.2)
26	1349.0 (1343.7)	61.3 (63.7)	26	1030.5 (1029.3)	1.2 (1.0)	1043.4 (1037.9)	2.6 (1.4)
27	1454.6 (1442.2)	25.5 (19.0)	27	1076.4 (1072.6)	11.9 (9.6)	1085.1 (1080.5)	0.2 (0.2)
28	1479.8 (1470.2)	211.8 (212.4)	28	1238.3 (1234.2)	164.9 (104.5)	1250.8 (1242.7)	6.1 (2.4)
29	1523.9 (1515.3)	139.4 (144.4)	29	1244.4 (1237.0)	2.2 (3.4)	1253.5 (1245.5)	4.5 (5.3)
30	1540.4 (1533.9)	116.5 (133.8)	30	1277.7 (1268.8)	194.2 (163.3)	1300.9 (1289.1)	91.2 (67.6)
31	1618.6 (1612.0)	108.1 (91.9)	31	1310.2 (1303.0)	166.5 (207.9)	1334.5 (1326.9)	242.9 (235.7)
32	1664.7 (1655.6)	1.6 (8.5)	32	1360.8 (1352.5)	49.0 (41.3)	1355.6 (1348.5)	8.6 (12.7)
33	1675.2 (1672.6)	208.7 (202.7)	33	1452.9 (1441.7)	148.8 (7.3)	1457.5 (1445.7)	60.9 (43.0)
34	3163.0 (3147.3)	6.4 (5.7)	34	1455.4 (1446.0)	50.8 (190.6)	1487.0 (1474.7)	168.4 (171.9)
35	3172.0 (3156.2)	3.7 (2.9)	35	1524.7 (1516.0)	103.2 (89.2)	1515.8 (1508.6)	254.5 (260.6)
36	3186.3 (3171.7)	12.2 (7.7)	36	1535.4 (1529.2)	68.5 (86.0)	1539.1 (1532.5)	107.9 (112.4)
37	3193.2 (3176.9)	15.2 (9.7)	37	1605.8 (1596.1)	376.1 (407.9)	1602.9 (1596.3)	178.8 (170.2)
38	3198.2 (3184.1)	8.3 (8.2)	38	1651.0 (1639.5)	30.3 (59.2)	1661.0 (1651.5)	37.5 (71.5)
39	3331.6 (3337.3)	132.8 (143.5)	39	1665.6 (1645.3)	161.1 (8.2)	1668.0 (1662.8)	168.8 (159.1)
			40	1686.8 (1661.5)	61.7 (139.4)	1707.7 (1672.1)	58.0 (10.0)
			41	3162.1 (3146.3)	8.1 (6.8)	3167.3 (3150.9)	5.2 (5.1)
			42	3170.5 (3154.7)	4.5 (3.2)	3174.6 (3158.8)	6.7 (4.7)
			43	3186.0 (3170.1)	8.7 (4.4)	3188.7 (3173.4)	13.0 (8.7)
			44	3190.4 (3173.3)	15.0 (11.4)	3196.6 (3179.6)	3.9 (0.0)
			45	3198.1 (3184.4)	15.1 (11.8)	3200.4 (3184.9)	11.7 (11.4)
			46	3324.9 (3350.0)	988.1 (930.8)	3368.0 (3391.1)	165.2 (178.5)
			47	3602.7 (3604.2)	451.6 (680.8)	3556.7 (3593.7)	607.1 (650.2)
			48	3813.4 (3879.5)	129.9 (104.9)	3825.2 (3894.7)	106.9 (92.9)
	H ₂ O						
	Frequency	Intensity					
1	1666.4 (1636.4)	99.9 (84.7)					
2	3726.9 (3816.9)	6.6 (6.5)					
3	3851.1 (3925.5)	53.1 (56.3)					

^aValues are calculated at the Becke3LYP/6-31+G* level of theory while those in parentheses are results from the Becke3LYP/6-31+G'[2d,p] level of theory. All frequencies are given in wave numbers.

frequency is not expected to change much between the two structures, despite the very different mode of binding, and indeed the frequency shifts are close to one another and to experiment.

It is more surprising that the water H-bonded OH and tropolone OH frequencies for the two isomers are so similar to one another. This is most notable in the tropolone OH stretch, where it might have been anticipated that the partial

disruption of tropolone's intramolecular H bond by water in isomer I would have a significant effect on its vibrational frequency. However, the weakening of the intramolecular H bond is compensated by additional H bonding to the water molecule, resulting in a TrOH OH vibrational frequency quite close to that of TrOH itself.

(b) The OH bending mode of water in the complex is at 1600 cm⁻¹, 5 cm⁻¹ blue shifted from its fundamental fre-

TABLE IV. Overlap coefficients between the normal modes of tropolone and water^a and those of two TrOH·H₂O conformers.^b

Spectroscopic identification	Frequency (cm ⁻¹)	Mode number	Ring isomer of TrOH·H ₂ O				Exterior isomer of TrOH·H ₂ O			
			Mode (freq) ^c	O.C.	Mode (freq) ^c	O.C.	Mode (freq) ^c	O.C.	Mode (freq) ^c	O.C.
TrOH ν_{26}	114.9	1	2 (84.1)	0.978			4 (119.4)	0.942		
TrOH ν_{25}	185.1	2	5 (183.4)	0.986			6 (187.7)	0.998		
TrOH ν_{14}	363.4	3	7 (329.5)	0.455	10 (382.6)	0.751	7 (368.3)	0.849	8 (381.6)	0.507
	373.9	4	8 (358.3)	0.646	10 (382.6)	0.560	7 (368.3)	0.494	8 (381.6)	0.814
TrOH ν_8	1324.9	25	31 (1310.2)	0.801			31 (1334.5)	0.900		
TrOH ν_{27}	3331.6	39	46 (3324.9)	0.980			46 (3368.0)	0.999		
H ₂ O ν_2	1667.1	1	40 (1686.8)	0.948			40 (1707.7)	0.967		
H ₂ O ν_1	3728.8	2	47 (3602.7)	0.864	48 (3813.4)	0.493	47 (3556.7)	0.842	48 (3825.2)	0.537
H ₂ O ν_3	3852.4	3	47 (3602.7)	0.482	48 (3813.4)	0.870	47 (3556.7)	0.537	48 (3825.2)	0.844

^aThe water and tropolone monomers were overlapped with their respective species in the conformer.

^bVibrational frequencies were calculated at the Becke3LYP/6-31+G* level of theory.

^cNormal mode numbers given correspond to those listed in Table III while calculated frequencies (in cm⁻¹) are given in parentheses.

quency in the free water molecule (1595 cm⁻¹). The *ab initio* calculations predict small blue shifts for both isomers, of somewhat greater magnitude than observed experimentally. In the exterior isomer, the comparison is somewhat less clear because two modes carry significant OH bend character. Nevertheless, a small blue shift in the bending mode is expected for water molecules which are acting as a hydrogen bond donor. For instance, in the water dimer in a matrix,²⁰ the bending mode of the donor water molecule is at 1599.2 cm⁻¹. Since both TrOH·H₂O structures have the water molecule as a hydrogen-bond donor, it is not surprising that blue shifts are predicted by both calculations.

(c) Several low frequency intramolecular modes of tropolone in the TrOH·H₂O complex have been clearly assigned from the dispersed emission studies of Sekiya *et al.*² Of these, the C–O stretch (1283 cm⁻¹, ν_8) and the in-plane symmetric O–O wag (372 cm⁻¹, ν_{14}) have frequency shifts of more than 10 cm⁻¹ to the blue relative to TrOH. In phenol, the frequency of the C–O stretch blue shifts when the COH group acts as proton donor. As shown in Table IV, in TrOH·H₂O, both ν_8 and ν_{14} are calculated to have some mixing with other modes induced by complexation with water. Nevertheless, the dominant mode character can be easily identified and serves as the basis for the frequency shifts reported in Table V. For ν_8 , both the ring and exterior isomers are calculated to have blue shifts, though the magnitude of the shift for the ring isomer is considerably larger, as might be expected. The magnitude of the blue shift is better matched by the exterior isomer, but no clear distinction can be made on this basis. In ν_{14} , only the exterior isomer has the correct direction of the shift, though the calculated mixing with other modes is extensive enough that a firm differentiation between the two structures on this basis cannot be made.

The low-frequency out-of-plane ring mode ν_{25} (173 cm⁻¹) is not changed by complexation, but neither is either isomer calculated to have a significant frequency shift in ν_{25} .

(d) Sekiya and co-workers² assigned the ground-state intermolecular stretch at 145 cm⁻¹, a value reasonably reproduced by the calculations for both isomers (144 and 166 cm⁻¹ at Becke3LYP 6-31+G*).

2. Evidence for the ring isomer

Evidence for the ring isomer is given in more detail in the following paper by Mitsuzuka *et al.*³ Here we briefly summarize those points of most direct relevance to our data.

(a) The ground state pK_a of tropolone²¹ is 6.7, indicating that tropolone is a better acid than water (in aqueous solution) and hence would be expected to be a better proton donor than acceptor in the hydrogen-bonded complex with water. The ring isomer incorporates tropolone as a proton donor to water.

(b) As with aromatic alcohols, the excited state acidity of tropolone is much lower than that of the ground state. This would suggest an even stronger propensity for the ring isomer over the exterior isomer in the S_1 state. In the absence of a barrier between these two structures, if the exterior isomer is favored in the ground state, but the ring isomer in the excited state, electronic excitation would lead to long progressions in intermolecular modes in the electronic spectrum with maxima away from the origin transition, counter to observation.

(c) While the vibrational frequency shift of the TrOH OH stretch absorption in TrOH·H₂O is not so different than that of TrOH, the absorption is significantly broader and more complex in TrOH·H₂O than in TrOH, suggesting significant interactions of water with the TrOH OH. This is more easily understood if the water molecule is in the ring structure than in the exterior structure.

3. Evidence for the exterior isomer

The evidence for the exterior isomer is as follows.

(a) The S_0 – S_1 frequency shift to the blue (+286 cm⁻¹) is in the opposite direction expected for the ring structure in which the OH of tropolone acts as a proton donor to water. Since the electronic frequency shift is a direct measure of the difference in binding energies between the S_1 and S_0 states, i.e.,

$$\Delta\nu = D_0(S_0) - D_0(S_1),$$

TABLE V. Comparison of the experimental vibrational frequencies and frequency shifts with those calculated for a select set of vibrations in the ring and exterior isomers of TrOH-H₂O. All values are given in wave numbers.

Mode	Tropolone		Tropolone-H ₂ O		
	Expt.	Calc. ^a 6-31+G*/ 6-31+G'[2 <i>d</i> , <i>p</i>]	Expt.	Ring calc. ^a 6-31+G*/ 6-31+G'[2 <i>d</i> , <i>p</i>]	Exterior calc. ^a 6-31+G*/ 6-31+G'[2 <i>d</i> , <i>p</i>]
H ₂ O Free OH					
ν_{free}			3724	3813/3880	3825/3895
$\Delta\nu_{\text{free}}^{\text{b}}$			+18	+23/+8	+34/+23
H ₂ O H-bonded OH					
$\nu_{\text{H bond}}$			3506	3603/3604	3557/3594
$\Delta\nu_{\text{H bond}}^{\text{b}}$			-200	-188/-267	-234/-277
H ₂ O bend					
ν_{bend}			+1600 ^g	1687/1662	1708/(1652,1663)
$\Delta\nu_{\text{bend}}^{\text{b}}$			+5	+20/+26	+41/(+16,+27)
TrOH OH					
ν_{TrOH}	3137	3332/3337	~3150-3200	3325/3350	3368/3391
$\Delta\nu_{\text{TrOH}}^{\text{c}}$			~+13-+63	-7/+13	+36/+54
TrOH C-O stretch					
ν_8	1269	1325	1283	1310/	1334/1327
$\Delta\nu_8^{\text{c}}$			+14	-15/	+9/+6
In-plane O-O wag ^d					
$\nu_{14}(S_0)$	359	363/359		383/380	368/366
$\Delta\nu_{14}^{\text{c}}$			+11	+20/+21	+5/+7
ν_{25}	173	185/184	173	183/182	188/184
$\Delta\nu_{25}^{\text{c}}$			0	-2/-1	+3/0
ν_{26}	111	115/121	109	84/87	119/120
$\Delta\nu_{26}^{\text{c}}$			-2	-31/-34	+4/-1
Intermolecular Modes ^e					
Out-of-plane bend			33 ^f	50/50	42/h
β (in-plane bend)			58 ^f	175/167	69/h
$\Delta\nu_{\beta}$				+106/+98	0/h
σ (stretch) ^f			145	144/118	166/h
$\Delta\nu_{\sigma}$				-1/-27	+21/h

^aVibrational frequencies using density functional theory with Becke3LYP functionals and either a 6-31+G* or 6-31+G'[2*d*,*p*] basis set, as described in the text.

^bRelative to the free OH stretch in the H₂O monomer: In the calculations, taken as the average of the symmetric and antisymmetric stretch modes of H₂O at the same level of calculation. Experimentally, this average is $\frac{1}{2}(3657+3756)=3706 \text{ cm}^{-1}$.

^cRelative to the corresponding vibration in the tropolone monomer.

^d ν_{14} undergoes significant mixing with other nearby modes upon complexation with water, particularly in the ring isomer. The frequencies and frequency shifts given are for the mode with largest overlap with ν_{14} in tropolone.

^eThe nature of the intermolecular modes changes somewhat between ring and exterior isomers. The designation gives the major motion, but assignments as bend, stretch, or torsion are only approximate. Out-of-plane and in-plane refer to the plane of tropolone which is a true symmetry plane for the exterior isomer, but only an approximate symmetry plane in the interior isomer.

^fExperimental frequencies and assignments taken from Ref. 2. In Ref. 2, the out-of-plane bend is assigned as the β_2^1 overtone at 66 cm^{-1} . The present data suggests a possible reassignment of the in-plane bend as 66 cm^{-1} .

^gDetermined from the combination band built off the free OH at 5324 cm^{-1} ($3724+1600$).

^hThe optimization of the exterior structure with the 6-31+G'[2*d*,*p*] basis set used a convergence criterion which gave one negative frequency in the intermolecular modes. Hence, these numbers are not included in the table.

the experimental blue shift indicates a decrease in the binding energy in the S_1 state. Yet, the increased acidity of the S_1 state should strengthen the hydrogen bond to water in the ring structure, yielding a red shift. For instance, the phenol-H₂O complex, which has a structure in which phenol acts as proton donor to water, possesses an electronic frequency shift of -353 cm^{-1} . At the same time, the blue shift of the exterior isomer is qualitatively reproduced by the increased HOMO-LUMO gap calculated for the exterior isomer ($+599 \text{ cm}^{-1}$ with the MP2 6-31+G[2*d*,*p*] basis set),

while a red shift is predicted (-423 cm^{-1}) for the ring isomer. The HOMO-LUMO gap has been effective in reproducing qualitative experimental frequency shifts in other aromatic clusters.²²

(b) Quantitative comparisons of the OH stretch infrared intensities with the *ab initio* predictions is hindered by the wavelength-dependent OPO power and the possibility of changing beam overlap over large frequency ranges. Given their close proximity, perhaps the most reliable comparison can be made between the ratios of total integrated intensities

of the C–H stretch and TrOH OH stretch bands, i.e., $I_{\text{TrOH}}/I_{\text{C-H}}$. The experimental value for this ratio is $I_{\text{TrOH}}/I_{\text{CH}}(\text{expt.})=3$.

For the exterior isomer, this ratio is predicted by calculation to be changed only modestly (~50%) from its value in tropolone by virtue of the water molecule not directly disturbing the intramolecular hydrogen bond. However, as seen in Table III, the ratio is calculated to increase dramatically in the ring isomer where tropolone's OH forms an intermolecular hydrogen bond with water, with a calculated ratio of $I_{\text{TrOH}}/I_{\text{CH}}(\text{ring})=25$, far in excess of the experimental result. As has been noted previously, this intensity increase is characteristic of intermolecular hydrogen bond formation.^{14,23} For instance, the recent measurements of Ebata *et al.*¹⁴ show that phenol's OH stretch intensity is increased by a factor of 6 when it hydrogen bonds to water.

(c) In the $S_1 \leftarrow S_0$ spectrum of tropolone, ν_{26} , an out-of-plane, out-of-phase wagging vibration of the oxygen atoms, exhibits a long progression in its even overtones.^{24,25} Sekiya and co-workers² have assigned the analogous vibration in TrOH-H₂O by virtue of its near-identical frequency (109 cm⁻¹) and intensity profile relative to TrOH (111 cm⁻¹). As expected, the exterior isomer is also calculated to have a very small frequency shift in ν_{26} (-1 cm⁻¹). However, the ring isomer is predicted to have a frequency of only 87 cm⁻¹ ($\Delta\nu=-34$ cm⁻¹) due to the increased effective mass for the vibration with water attached to both oxygens involved in the out-of-plane motion.

(d) Sekiya *et al.*² have observed peaks in the single vibronic level S_1 emission spectra at 57 and 69 cm⁻¹ from the origin, and have assigned the transitions to the intermolecular bending modes. If these assignments are correct, the presence of two low-frequency bending modes supports the exterior structure, since the ring isomer has a calculated in-plane bending fundamental almost 100 wave numbers higher (167 cm⁻¹).

(e) Finally, the exterior isomer is calculated to be the more stable conformer both with and without zero-point energy and BSSE corrections for both Becke3LYP and MP2 calculations.

The body of evidence does not present an overwhelming case for one isomer over the other. Taken as a whole, it appears to us that the exterior isomer is somewhat preferred by the present data. Nevertheless, a high-resolution frequency domain or rotational coherence measurement is needed to conclusively answer the question. The rotational constants listed in Table II would suggest a clear distinction between the two structures from the rotational data.

B. The breadths and substructure of the TrOH-H₂O OH stretch bands

The juxtaposition of an intramolecular H bond, an intermolecular H bond, and a free OH in the TrOH-H₂O complex presents an opportunity for direct comparison of their spectral consequences. Since intensity comparisons between intramolecular and intermolecular H bonds have already been discussed in the preceding paper on TrOH,⁵ the primary

point of concern here is with the observed breadths and substructure of the bands. Nevertheless, it is worth noting that the qualitative differences between the frequency shifts and intensities of intramolecular and intermolecular H bonds are borne out by the present data. The intramolecularly H-bonded tropolone OH, despite having a much lower frequency than the intermolecularly H-bonded OH on water, has an integrated band absorbance which is only about one-fourth the latter's intensity.

The widths and substructure of the three OH stretch bands in TrOH-H₂O are also highly mode specific and clearly run counter to density-of-states arguments. The least strongly mixed level [free OH($\nu=1$)] is highest in energy (where the density of states is greatest), while the most strongly mixed level [tropolone OH($\nu=1$)] is lowest in energy (where the density of states is smallest).

The narrow bandwidth and uncongested surroundings of the free OH stretch band is consistent with the weak coupling expected for the free OH to other modes in the complex. The two weak combination bands built off the free OH stretch (at 3797 and 5324 cm⁻¹) are also quite sharp and largely uncongested. The 5324 cm⁻¹ band is the water free OH/intramolecular water bend combination band, and is no more than a few wave numbers from its value in the free water molecule.

The 73 cm⁻¹ shift of the 3797 cm⁻¹ band from the free OH stretch is very similar to the 69 cm⁻¹ interval seen in the combination band built off the water H-bonded OH stretch. As already mentioned, Sekiya *et al.*² have observed intermolecular bands at 57 and 66 cm⁻¹ in the dispersed emission from tropolone-H₂O. They assign the 57 cm⁻¹ band to the intermolecular in-plane bend, α_1^0 , and the 66 cm⁻¹ transition to the overtone of the out-of-plane bend, β_2^0 . It is unlikely that our observed combination bands are $|v_{\text{OH}}=0, v_{\beta}=0\rangle \rightarrow |v_{\text{OH}}=1, v_{\beta}=2\rangle$, since the corresponding transition to $|v_{\text{OH}}=1, v_{\beta}=1\rangle$ is not observed. An assignment as the $|v_{\text{OH}}=0, v_{\alpha}=0\rangle \rightarrow |v_{\text{OH}}=1, v_{\alpha}=1\rangle$ combination band seems more likely, though this would necessitate either a 12 cm⁻¹ increase in the in-plane bend frequency upon OH stretch vibrational excitation or a reversal of Sekiya's assignments of the in-plane and out-of-plane progressions.

Intensity in combination bands can arise from electrical anharmonicity, mechanical anharmonicity, or large-amplitude motions. In a moderate-strength hydrogen bonded complex such as this, mechanical anharmonicity should not be particularly great, and electrical anharmonicity involving ($\partial^2\mu/\partial Q_{\text{OH}}\partial Q'$) seems a more likely source of combination band intensity. For the free OH/intramolecular water bend combination band at 5324 cm⁻¹, such electrical anharmonicity would seem quite reasonable, even in the absence of complexation of water to tropolone.

It is more surprising that of the six intermolecular modes in the complex, only the hydrogen-bond bending mode at 69 cm⁻¹ carries intensity in a combination band. Notably, the H-bond stretch ($\sigma=145$ cm⁻¹ in S_0) shows no measurable intensity as a combination band with either the free OH or H-bonded water OH stretch. In several complexes possessing strong H bonds, combination bands involving the H-bond

stretch play a key role in determining the breadth and substructure in the OH stretch region.²⁶ This method for OH stretch band broadening is called the Sheppard effect,²⁷ in which the OH stretch/H-bond stretch combination bands gain intensity through the sensitive dependence of the force constant and dipole moment of the OH bond on the O···HO separation. The Sheppard effect is noticeably absent in the TrOH-H₂O hydrogen bond.

The combination bands involving the 69 cm⁻¹ H-bond bend may signal an unusually large cross-electrical anharmonicity ($\partial^2\mu/\partial Q_{\text{OH}}\partial Q_\alpha$). Alternatively, some of the intensity in the OH stretch/H-bond bend combination band may be a consequence of the large-amplitude motion of the intermolecular bend. The importance of large-amplitude motions (LAMs) in inducing intensity in combination bands was especially evident in the OH stretch infrared spectrum of the benzene-HOD complex²⁸ where the large-amplitude torsional motion of HOD led to OH stretch/torsion combination bands whose intensity actually exceeded that of the OH stretch fundamental. In the presence of LAM, the vector nature of the dipole moment function must be taken explicitly into account. If the LAM in vibration a is along the coordinate ρ , then

$$\begin{aligned} \langle v_{\text{OH}}=0, v_{\text{bend}}=0 | \left(\frac{\partial \tilde{\mu}(\rho)}{\partial Q_{\text{OH}}} \right) Q_{\text{OH}}(\rho) | v_{\text{OH}}=1, v_{\text{bend}}=1 \rangle \\ = \left(\frac{\partial \mu}{\partial Q_{\text{OH}}} \right)_0 \langle 00 | Q_{\text{OH}} \cdot \phi(\rho) | 11 \rangle \\ = \left(\frac{\partial \mu}{\partial Q_{\text{OH}}} \right)_0 \langle 0 | Q_{\text{OH}} | 1 \rangle \langle 0 | \phi(\rho) | 1 \rangle \\ \neq 0 \quad \text{for some } \phi(\rho). \end{aligned}$$

Here $\phi(\rho)$ describes the dependence of the OH bond as it undergoes the LAM along the in-plane bend ρ . If $\phi(\rho)$ changes significantly over the range of ρ probed during the vibration in ρ , intensity can be induced in combination bands involving the coordinate ρ .

Like the free OH, the water H-bonded OH is also dominated by a single transition [Fig. 5(a)], but several satellite bands only 13, 25, and 34 cm⁻¹ above it also appear. Relative to the fundamental water H-bonded OH transition, these satellite bands are quite weak [Fig. 5(b)], but on an absolute basis each of these bands is about one-half the intensity of the free OH fundamental after correction for laser power differences in the two regions. The source of these additional bands is particularly puzzling. Combination bands are not likely, since no vibrations in the complex should have such a low frequency. Fermi resonance mixing is more plausible, but we are unable to probe sensitively for analogous bands on the low frequency side of the fundamental due to the much lower OPO power in this region. Since the excitation frequency probably exceeds the binding energy of the complex, Fermi mixing would be to a small subset of the total density of states. Finally, the low-lying bands could result from coupling to levels involving H-atom transfer, whether in an asymmetric well, such as in the exterior isomer or in a

more complicated symmetric tunneling route in the ring isomer. The transition states associated with several of these tunneling pathways are currently being explored via *ab initio* methods.

Finally, in the tropolone OH stretch region, the absorption is at least 100 cm⁻¹ broad, but shows distinct, reproducible, but irregularly spaced substructure. The source of this structure is probably Fermi resonance mixing in which the OH stretch carries the oscillator strength and is mixed with a select subset of the total bath of dark background states at that energy. The most likely sources of this substructure are 2:1 Fermi resonances with the six modes in the 1500–1700 cm⁻¹ region (Table III). After anharmonic scaling (0.96), these six modes produce a set of 21 combinations and overtones with average spacing of about one state/15 cm⁻¹, in reasonable correspondence with experiment. Given the overall breadth of the band, the coupling matrix elements involved are about 100 times greater than that in the free OH region. Furthermore, the comparison with tropolone itself indicates that the state mixing present in the TrOH OH stretch region in TrOH-H₂O is significantly more extensive than that in tropolone itself.

VI. CONCLUSION

The comparison of *ab initio* results with the FDIR spectra of the TrOH-H₂O complex in the OH stretch region provides a clear juxtaposition of the spectral characteristics of a free OH, intermolecularly H-bonded OH, and an intramolecularly H-bonded OH. The breadths of the observed transitions are particularly striking, varying from the instrumentally limited sharpness of the free OH (1.8 cm⁻¹ FWHM) to the TrOH OH band spread over at least 100 cm⁻¹. The two lowest-energy isomeric structures calculated for the complex bind water on the exterior and interior (i.e., OH side) of the keto oxygen. While the binding position is quite different, the mode of binding is qualitatively similar in that both structures incorporate a free OH, water H-bonded OH, and TrOH OH. An extensive comparison of the spectroscopic data on TrOH-H₂O with the *ab initio* calculations does not provide a definite assignment for the experimentally probed structure, though the data is somewhat more consistent with the exterior structure. The present data clearly call for further experiments designed to answer this question unambiguously.

ACKNOWLEDGMENTS

The authors gratefully acknowledge the support of the National Science Foundation for this research. T.S.Z. also acknowledges the Petroleum Research Fund, administered by the American Chemical Society for their support. R.K.F. was supported by an industrial fellowship from Lubrizol. The authors gratefully acknowledge Professor Sekiya and Professor Mikami for providing the results of their work prior to publication. T.S.Z. also thanks Professor Mikami and his group for a wonderful visit to Sendai during which many fruitful discussions regarding the tropolone-H₂O complex occurred.

- ¹Y. Tomioka, M. Ito, and N. Mikami, *J. Phys. Chem.* **87**, 4401 (1983).
- ²H. Sekiya, H. Hamabe, N. Nakano, H. Ujita, N. Nakano, and Y. Nishimura, *Chem. Phys. Lett.* (in press).
- ³A. Mitsuzuka, A. Fujii, T. Ebata, and N. Mikami, *J. Chem. Phys.* **105**, 2618 (1996), following paper.
- ⁴R. L. Redington and C. W. Bock, *J. Phys. Chem.* **95**, 10284 (1991).
- ⁵R. K. Frost, F. Hagemester, C. A. Arrington, and T. S. Zwier, *J. Chem. Phys.* **105**, 2595 (1996), preceding paper.
- ⁶F. A. Ensminger, J. Plassard, T. S. Zwier, and S. Hardinger, *J. Chem. Phys.* **99**, 8341 (1993).
- ⁷F. A. Ensminger, J. Plassard, T. S. Zwier, and S. Hardinger, *J. Chem. Phys.* **102**, 5246 (1995).
- ⁸Z. S. Huang and R. E. Miller, *J. Chem. Phys.* **91**, 6613 (1989).
- ⁹F. Huisken, M. Kaloudis, and A. Kulcke, *J. Chem. Phys.* **104**, 17 (1996).
- ¹⁰R. N. Pribble and T. S. Zwier, *Science* **265**, 75–79 (1994).
- ¹¹R. N. Pribble and T. S. Zwier, *Faraday Discuss.* **97**, 229 (1994).
- ¹²T. S. Zwier, *Annu. Rev. Phys. Chem.* (1996), Vol. 47, p. 205.
- ¹³S. Djafari, G. Lembach, H.-D. Barth, and B. Brutschy, *Z. Phys. Chem.* (in press).
- ¹⁴T. Ebata, T. Watanabe, and N. Mikami, *J. Phys. Chem.* **99**, 5761 (1995).
- ¹⁵GAUSSIAN 94, Revision A.1, M. J. Frisch, G. W. Trucks, H. B. Schlegel, P. M. W. Gill, B. G. Johnson, M. A. Robb, J. R. Cheeseman, T. A. Keith, G. A. Petersson, J. A. Montgomery, K. Raghavachari, M. A. Al-Laham, V. G. Zakrzewski, J. V. Ortiz, J. B. Foresman, J. Cioslowki, B. B. Stefanov, A. Nanayakkara, M. Challacombe, C. Y. Peng, P. Y. Ayala, W. Chen, M. W. Wong, J. L. Andres, E. S. Replogle, R. Gomperts, R. L. Martin, D. J. Fox, J. S. Binkley, D. J. Defrees, J. Baker, J. P. Stewart, M. Head-Gordon, C. Gonzalez, and J. A. Pople, Gaussian, Inc., Pittsburgh, PA, 1995.
- ¹⁶C. Möller, M. S. Plesset, *Phys. Rev.* **46**, 618 (1934); R. J. Bartlett, *Annu. Rev. Phys. Chem.* **32**, 359 (1981).
- ¹⁷(a) A. D. Becke, *J. Chem. Phys.* **98**, 5648 (1993); (b) S. H. Vosko, L. Wilk, M. Nusir, *Can. J. Phys.* **58**, 1200 (1980); (c) C. Lee, W. Yang, and R. G. Parr, *Phys. Rev. B* **37**, 785 (1988).
- ¹⁸S. F. Boys, F. Bernardi, *Mol. Phys.* **19**, 553 (1970).
- ¹⁹(a) K. Kim, K. D. Jordan, and T. S. Zwier, *J. Am. Chem. Soc.* **116**, 11568 (1994); (b) S. Y. Fredericks, K. D. Jordan, and T. S. Zwier, *J. Phys. Chem.* (in press).
- ²⁰D. Forney, M. E. Jacox, and W. E. Thompson, *J. Mol. Spectrosc.* **157**, 479 (1993).
- ²¹E. F. Breheret and M. M. Martin, *J. Lumin.* **17**, 49 (1978).
- ²²(a) M. Pohl, M. Schmitt, K. Kleinermanns, *J. Chem. Phys.* **94**, 1717 (1991); (b) V. Brenner, S. Martenchar-Barra, P. Millie, C. Dedonder-Lardeux, C. Jouvet, and D. Solgadi, *J. Phys. Chem.* **99**, 5848 (1995).
- ²³G. C. Pimentel and A. L. McClellan, *The Hydrogen Bond* (Freeman, San Francisco, 1960).
- ²⁴H. Sekiya, Y. Nagashima, and Y. Nishimura, *J. Chem. Phys.* **92**, 5761 (1990).
- ²⁵R. L. Redington, Y. Chen, G. J. Scherer, and R. W. Field, *J. Chem. Phys.* **88**, 627 (1988).
- ²⁶(a) A. C. Legon and D. J. Millen, *Chem. Rev.* **86**, 635 (1986), and references therein; (b) D. J. Millen, *J. Mol. Struct.* **100**, 351 (1983).
- ²⁷N. Sheppard, in *Hydrogen Bonding*, edited by D. Hadzi (Pergamon, New York, 1959), p. 85.
- ²⁸R. N. Pribble, A. W. Garrett, K. Haber, and T. S. Zwier, *J. Chem. Phys.* **103**, 531 (1995).